Supporting Information

Engineering Hetero-structural Iron Nanozymes Decorated Liposome with Self-Cascade Catalysis Performance

Teng Wang, [†ab] Qing Wu, [†ab] Zhenyu Wang, [†ab] Xi Hu, [ab] Xiang Mao [*ab]

a. State Key Laboratory of Ultrasound in Medicine and Engineering, College of Biomedical Engineering, Chongqing Medical University, Chongqing 400016, China

b. Chongqing Key Laboratory of Biomedical Engineering, College of Biomedical Engineering, Chongqing Medical University, Chongqing 400016, China

Materials and methods

1. Materials

Polydimethylsiloxane (PDMS) was purchased from Dow Corning (Midland, MI, USA). Iron (II) chloride tetrahydrate ($FeCl_2 \cdot 4H_2O$, 98%) and Span 80 were obtained from Sigma-Aldrich Co., Ltd. (St. Louis, MI, USA). Oleic acid (OA, 99%) was purchased from Sigma-Aldrich (St. Louis, MO). Iron chloride hexahydrate ($FeCl_3 \cdot 6H_2O$, 99%), Glycerol (99%, 92.09 (MW)), Poly (vinyl alcohol) (PVA, 87%-89% hydrolyzed, 44.05 (MW)), cholesterol, Sodium citrate tribasic dihydrate ($C_6H_5Na_3O_7 \cdot 2H_2O$, ≥99%), Polyethyleneimine ethylenediamine branched (PEI, average weight 800), 3,3',5,5'-Tetramethylbenzidine (TMB, 240.35 (MW)) Glucose Oxidase from Aspergillus niger (GOx, 100 U/mg), Dimethyl sulfoxide (DMSO, 78.13 (MW)), Phosphate buffer (pH 5.8), phosphate-buffered saline (PBS, pH 7.4) were produced by Aladdin Reagent Co., Ltd. (Shanghai, China). Fluoresent molecular probes (3,3'-diocyadecyloxacarbocyanine perchlorate, Dio, ex/em 484/501 nm) were purchased from Beyotime Biotechnology (Shanghai, China). D-Glucose ($C_6H_{12}O_6 \cdot H_2O$, 198.17 (MW)) and Sucrose ($C_{12}H_{22}O_{11}$, 342.30 (MW)) were provided by KESHI (Chengdu, China). Pluronic F-68 was provided by gibco (thermofisher, USA). Sliver acetate ($C_2H_3O_3Ag$, 99.5%) was produced bymacklin (Shanghai, China). Hydrogen peroxide (H_2O_2, 30%) and Ammonium hydroxide solution ($NH_3 \cdot H_2O$) were purchased from Chuandong chemical industry (Chongqing, China). Soy Phosphatidylcholine (SPC, 95%) was purchased from Avanti Polar Lipids (Alabaster, AL).

2. Characterizations

Transmission electron microscopy (TEM) on an FEI TF 20 Super-X was used to examine the sample's morphology and particle size. The sample was dropped vertically onto a carbon film that had been placed on a piece of clean, dry filter paper, and was then given 30 seconds to stand. A filter paper was used to carefully drain the extra liquid. Three times, the aforementioned steps were repeated. The carbon film was then left for 24 hours in a windless and dust-free environment. Ultraviolet–visible–near infrared (UV-vis-NIR) diffuse reflectance spectra were employed to investigate the

optical properties of different samples on a UV−3600i Plus UV-vis spectrometer. The zeta potential of each sample was measured by dynamic light scattering (DLS) using a zeta sizer Nano-Brook Omni (Brookhaven Instruments, Billerica, MA, USA). The prepared sample was diluted 10-fold with deionized water. The measurement conditions were room temperature of 25 ℃ and a detector angle of 90°. Ultraviolet absorption spectrum was detected using a UV−3600i Plus UV-vis spectrometer. For this, 3 mL sample was taken in a quartz cuvette and the scanning range was 300-800 nm with a medium scanning speed. Fourier Transform Infrared (FT-IR) spectroscopy was used to determine the chemical structure of the samples with Thermo Fisher Nicolet iS50 in the range of 400 cm^{-1} to 4000 cm^{-1}. A vibrating sample magnetometer (VSM) from Quantum Design PPMS−9 was used to measure the magnetic properties of the synthesized nanocomposite. The pH values were recorded using a pH meter (Mettler Toledo Five Easy Plus, Switerland). Thermogravimetric curves were obtained from thermogravimetric analysis instrument (NETZSCH TG 209F1 Libra, Germany) from 30 ℃ to 800 ℃ in nitrogen.

3. Preparation of Fe_3O_4@Ag structures.

Firstly, Fe_3O_4 nanoparticles were prepared via a chemical co-precipitation method, with slight changes. Briefly, $FeCl_2.4H_2O$ (0.19881 g) and $FeCl_3 \cdot 6H_2O$ (0.5406 g) were solved in 100 mL deionized water with a molar ratio of 1:2 in a triple-neck round-bottom flask. Following by a 20-minute sonication. The reaction temperature was then raised to 80 ℃ in a water bath, and the solution was allowed to react for 30 minutes while being continuously stirred magnetically. In the middle of the process, when water reached 30 ℃, add 8 mL ammonium hydroxide solution, when the water reached 40 ℃, add 2.94 g sodium citrate tribasic dihydrate ($C_6H_5Na_3O_7 \cdot 2H_2O$). After cooling the reaction mixture to room temperature, a black precipitate was obtained that was thoroughly washed several times with deionized water. A permanent magnet was used to separate the precipitate from the supernatant following each wash stage. Finally, the dark precipitate was dried for another application in a vacuum oven at 60 ℃ overnight.

In this work, the Fe_3O_4@Ag structures were synthesized using a “layer-by-layer”

method follows the previous experimental results of our research group, which comprised the formation of silver seeds on the surface of Fe_3O_4@PEI NPs and the formation of silver nanoparticles reduced by glucose. Firstly, Fe_3O_4 (0.0578 g) and glucose (2.25 g) were dissolved in 40 mL deionized water in a triple-neck round-bottom flask, then sonicated for 20 minutes. The reaction temperature was then increased to 100 ℃ after the mixture was heated and agitated in a water bath. The combination was given 10 mL PEI aqueous solution (0.1 $g \cdot mL^{-1}$). After 30 min, 10 mL of silver acetate was added to the mixture. With slow magnetic stirring, the reaction temperature was held at 100 ℃ for 2 h. After that, heating was turned off, and the mixture was stirring continuously until it cooled to room temperature. The items were gathered using a magnet and repeatedly cleaned with Milli-Q water. Finally, the dark precipitate was dried for an additional day at 37 ℃ in a vacuum oven.

4. Structure of ultrasound-integrated microfluidic device

As shown in Scheme 1a, the experimental device consisted of a microfluidic chip and an ultrasonic transducer. On the one hand, the microfluidic chip could be vertically divided into three parts: bottom glass layer, PDMS single-layer and top glass layer. The three parts were bonded together after plasma surface treatment. On the other hand, the microfluidic chip was composed of four parts horizontally: the Primary Assembly Channel, the Secondary Assembly Channel, the Ultrasonic Mixing channel and the Storage Chamber. The ultrasonic generator was composed of a power drive circuit and a bulk acoustic wave generator. Furthermore, it was composed of a piezoelectric ceramic chip with a power of 1 W, a frequency of 1 MHz and a matching drive circuit.

5. Fabrication of PDMS microfluidic device

The microfluidic chip was fabricated on substrates of polydimethylsiloxane (PDMS) via soft lithography and SU-8 photoresist molds. Using AutoCAD (Autodesk) to design the geometrical shapes and dimension of the microfluidic channels. The PDMS monomer and curing agent were mixed uniformly at a mass ratio of 10:1. The mixture was degassed and poured onto a silicon wafer with a microchannel mold, and then placed it at 65 ℃ for 2 h. The inlet and outlet of the channel were formed by using a biopsy punch through the PDMS layer. The PDMS layer was peeled off from the

mold, and the PDMS layer was bonded to the glass slide by oxygen plasma surface activation, then placed it at 200 ℃ for 90min to make the bonding closer. The channels for preparing liposomes were double-T type, since PDMS was hydrophobic, the surface of the second T-channel was treated to make it hydrophilic before use. The specific process was as follows: The external aqueous phase was filled with 3 wt.% PVA, and the inner aqueous phase and oil phase were filled with deionized water. After 10 minutes, the microfluidic chip was placed on the heating plate and dried at 75 ℃ for 15 minutes, and then the three phases were filled with deionized water for 5 minutes to ensure that the channel was unblocked.

6. The preparation of Soy Phosphatidylcholine (SPC) liposomes by microfluidic

The preparation of SPC liposomes was completed in the secondary assembly channel. In short, the internal water phase was a mixture of 5% Pluronic F-68 and sucrose solution. The oil phase consisted of phospholipid solution, cholesterol, Span 80 (25 $mg \cdot mL^{-1}$) and Dio (2 $\mu L \cdot mL^{-1}$), the phospholipid Soy Phosphatidylcholine was dissolved at a concentration of 5 mg/mL in oleic acid, the ratio of cholesterol to phospholipid is 1:2. The external water phase was composed of a mixture of 6% F-68 and glycerin. Adjusted the water phase flow rate to 10 $\mu L \cdot h^{-1}$, the flow rate ratio of oil phase to internal water phase was 1.5:1, and the flow rate ratio of external water phase to internal water phase was 30:1. Eventually, homogeneous Water/oil/Water (W/O/W) droplets would be generated.

7. The Synthesis of Soy Phosphatidylcholine/Fe_3O_4@Ag/GOx (SFAG) by Ultrasound-Integrated Microfluidic Device

Firstly, the microfluidic chip as shown in Scheme 1b, in the Primary Assembly Channel, the Fe_3O_4@Ag suspended solution and GOx solution were input through three injection ports with a diameter of 3 mm, and preliminarily mixed through S-shaped microchannels (0.1 mm width) to form Fe_3O_4@Ag/GOx nanoparticles (FAG NPs). At the same time, in the Secondary Assembly Channel was a dual T-type microchannels, which had three injection ports (3 mm diameter): the inner water phase, oil phase and outer water phase, respectively. Soy Phosphatidylcholine (SPC) liposomes were produced in the dual T-type microchannels. By adjusting the fluid

speed, SPC liposomes with three layers of water in oil and water could be formed step by step. Then the FAG NPs and SPC liposomes reached to the ultrasonic mixing channel which was a special micro mixing channel.

This mixing channel, which with the diameter of 13 mm and height of 4.5 mm, was covered with ITO glass and the ultrasonic piezoelectric ceramic chips in turn. Driven by the circuit, piezoelectric ceramic chip generates bulk acoustic wave in the chamber, which forms acoustic radiation force and acoustic flow effect in the whole chamber. The acoustic radiation force (F_{rad}) acted on the liposomes, making the liposomes uniformly arranged at the sound pressure nodes. When the liposomes dimeter was greater than 5 um,[1] its movement was dominated by the F_{rad}, which mainly influenced the movement of liposomes at the Y-Z plane. Accordingly, the F_{rad} could be controlled accurately by selecting the ultrasonic wavelength, power amplitude, and excitation source position. The drag force (F_{drag}) caused by the acoustic flow effect drives FAG NPs to accelerate disturbance, and constantly contacted with SPC liposomes which arranged in order. So that under the effect of electrostatic attraction and functional connection, SPC liposomes and FAG NPs formed a close connection, which was SFAG composite structure. Finally, the SFAG material was collected by the storage chamber (13 mm diameter, 4.5 mm height). The theoretical part of ultrasonic action was described in detail in the eighth part of ***Supporting Information***.

8. Ultrasound Theory and Parameter Screening

Ultrasonic manipulation of particles has the advantages of non-contact and no damage. The particles to be manipulated do not need to change their physical and chemical properties.[2-3] The physical basis of acoustic manipulation technology is ultrasonic force, which is generally divided into two types. The first is the force that the sound wave acts on the interface when there are different propagation media in the sound field. The second is the volume force of sound wave acting on the propagation medium in a uniform sound propagation medium, which can also be called the drag force caused by acoustic flow. For particles of micrometer and above size, the first acoustic radiation force (F_{rad}) generally plays a leading role; For nano particles, the

drag force (F_{drag}) caused by the acoustic flow, namely acoustic flow plays a leading role. [4]

For spherical SPC liposome with radius $R \ll \lambda$, the acoustic radiation force F_{rad} can be calculated with the Gor'kov potential in the acoustic domain[5-9]

$$F_{rad} = -\nabla\langle E\rangle \tag{1}$$

For the spatial energy density E can be expressed as:

$$E = 2\pi\rho_0 R^3\left(\frac{\langle p^2\rangle}{3\rho_0^2 c_0^2}f_1 - \frac{\langle v^2\rangle}{2}f_2\right) \tag{2}$$

Factor f_1 and f_2 depending on the mechanical properties of particles and fluid media, they can be expressed as:

$$f_1 = 1 - \frac{c_0^2\rho_0}{c_s^2\rho_s}, f_2 = 2\frac{\rho_s - \rho_0}{2\rho_s + \rho_0} \tag{3}$$

Where, p and v represent the value of the sound pressure and velocity respectively, ρ_0 and c_0 are the density and sound velocity of the medium, ρ_s and c_s represent the density and velocity of the particles. We uniformly use < > to represent the time average.

For Fe_3O_4@Ag/GOx (FAG) particles, the drag force (F_{drag}) plays a leading role. The governing equation of fluid motion can be expressed by the continuity equation and the Navier-Stokes equation as:[10-13]

$$\begin{gathered}\frac{\partial\rho}{\partial t} + \nabla(\rho\cdot v) = 0 \\ \rho\frac{\partial v}{\partial t} + \rho(v\cdot\nabla)v = -\nabla p + u\nabla^2 v_1 + \left(u_b + \frac{1}{3}u\right)\nabla(\nabla\cdot v)\end{gathered} \tag{4}$$

Where ρ is the mass density, v is the fluid velocity, p is the fluid pressure, μ is the dynamic viscosity, μ_b is the volume viscosity.

Nitesh Nama asume the relationship between P and ρ is linear:[14]

$$p = c_0^2\rho \tag{5}$$

c_0 is the speed of sound in the liquid at static.

The Nyborg perturbation theory is used to describe the mechanical coupling between the driving boundary and the fluid, in which it is assumed that the velocity, pressure and density of the fluid have the following forms:[15-16]

$$v = v_0 + v_1 + v_2$$

$$p = p_0 + p_1 + p_2 \tag{6}$$

$$\rho = \rho_0 + \rho_1 + \rho_2$$

The second order continuity equation and Navier Stokes equation are time averaged throughout the oscillation period. Angle brackets< >represent time averaged, where subscripts 0, 1 and 2 represent static, first order and second order quantities respectively. The second order continuity equation and the Navier-Stokes equation become the following forms:

$$\rho_0 \left(\nabla \cdot v_2\right) = -\nabla \left\langle \rho_1 v_1 \right\rangle$$

$$\left\langle \rho_0 \frac{\partial v_1}{\partial t} \right\rangle + \rho_0 \left\langle \left(v_1 \cdot \nabla\right) v_1 \right\rangle = -\nabla p_2 + u\nabla^2 \left\langle v_2 \right\rangle + \left(u_b + \frac{1}{3}u\right) \nabla \left(\nabla \cdot \left\langle v_2 \right\rangle\right) \tag{7}$$

From the above formula that the physical quantity of the first order sound field is taken as the source term of the second order sound flow field, and the driving force (ultrasonic volume force) of the sound flow can be expressed as:

$$f = - < \rho_1 \frac{\partial v_1}{\partial t} > - \rho_0 < (v_1 \cdot \nabla) v_1 > \tag{8}$$

In the acoustic flow field, when the flow rate is $< v_2 >$, the radius and speed of particles are α and μ. The average Stokes drag force F_{drag} given by:

$$F_{drag} = 6\pi\eta\alpha(< v_2 > - \mu) \tag{9}$$

9. Ultrasound Simulation Numerical Model

We established a simulation model by using the finite element software COMSOL Multiphysics 5.6 to simulate the movement of SPC liposomes in the sound field and the flow field. In order to simplify the calculation, the model was simplified to a two-dimensional model. The liquid was defined as water. The width of the model was 0.8

mm and the height was 1.5 mm. A 55 μm diameter microsphere model was placed in the water to replace the SPC liposome. The model was meshed. The calculation interface of the finite element model system was shown in Fig. 3. The upper and lower boundaries were set in the chamber as the incident pressure field, and the left and right boundaries were radiation boundaries. Using the laminar flow module coupled with the thermal viscous acoustic module, the first order velocity v_1 The boundary condition represented the ultrasonic piezoelectric transducer, simulated the drive of external ultrasonic, and simulated the frequency and power of external sound source by setting the boundary condition. In order to study the motion of the microspheres in the channel, the particle tracking module was used to simulate the trajectory and velocity of the particles. This module provided the Lagrange description of the particle motion, and the particle motion follows the Newton motion law. At the initial stage, the small balls were evenly distributed in the cavity.

To generate an ultrasonic field within the fluidic domain, a piezoelectric transducer was glued underneath the channel, transforming a sinusoidal voltage into mechanical vibration at a tunable frequency $f = \omega/(2\pi)$. This boundary the results in certain fluid resonance modes across the channel width w, when a traveling wave was superposed with a counter propagating reflected wave to result in a standing wave. Resonance occurs when a standing wave of $n \cdot \lambda/2 = \omega$. Fits between the reflecting left and right channel walls with $n = 1,2,3\ldots$ for the first, second and third harmonic and the acoustic wavelength λ.

10. Peroxidase-like activity measurement

The peroxidase-like activity of SFAG structure was examined utilizing TMB as chromogenic substrates in the presence of H_2O_2. By reacting with H_2O_2, the SFAG structure created enough ·OH to oxidize TMB into the TMB_{OX} blue product, as shown in Formula 1. Firstly, the pH range of SFAG structure and the stability of SFAG peroxidase-like activity of SFAG cascade enzyme at different concentrations were verified. The Michaelis-Menten equation was used to study the catalytic activity as shown in Formula 2 and Formula 3. The steady-state kinetic analysis experiment of

SFAG structure was carried out in time scanning mode in the UV spectrometer. In the reaction process, selecting one substrate of H_2O_2 and TMB as the variable, and keeping the concentration of the other substrate unchanged. Measure the UV absorbance of the product at 652 nm wavelength, and through transformation and calculation, Lineweaver-Burk curve can be obtained. Thus, the kinetic data Michaelis-Menten parameter (K_m), inversion-coefficient k_{cat} and maximum reaction speed V_{max} can be obtained. The specific reaction process was as follows: Add 100 μL (10 mM) H_2O_2 solution, 100 μL (10 mM) TMB solution and 100 μL (200 μg·mL^{-1}) SFAG solution to the 700 μL PBS (pH 7.4) respectively. After reaction enough then test the ultraviolet absorption of the product at 652 nm wavelength. and FAG NPs formed a close connection, which was SFAG composite structure. Finally, the SFAG material was collected by the storage chamber (13 mm diameter, 4.5 mm height). The theoretical part of

$$TMB_{OX} = \frac{A}{\sum_{[TMB_{OX}]} \times L} \tag{10}$$

$$\frac{1}{V_0} = \frac{K_m}{V_{max}[S]} + \frac{1}{V_{max}} \tag{11}$$

$$k_{cat} = \frac{V_{max}}{[S]} \tag{12}$$

where [TMB_{OX}] denotes the TMB_{OX} concentration, A is the UV-absorbance, L is the thickness (1 cm), and $\sum_{TMBox}$ shows the molar absorption coefficient, having the value of 39000 M^{-1}·cm^{-1} for the TMB_{OX} product at 652 nm. Under the calculation through equations, we can obtain the value of TMB_{OX}. Where V_0 represents the initial velocity, V_{max} refers to the maximum reaction velocity，and $[S]$ is the concentration of substrate.

10. Glucose detection real sample detection

As a sensor for glucose detection, SFAG complex enzyme could be detected in physiological pH buffer solution. The specific reaction process was that the GOx

enzyme in SFAG structure, as the first order enzyme, reacted with glucose to produce the intermediate product H_2O_2, the Fe_3O_4@Ag peroxidase-like enzyme which was then exposed on the SFAG surface reacts with H_2O_2 to produce ·OH, the ·OH oxidized TMB to produce dissociative and unstable TMB_{OX}, which was blue product, and the blue product combines with SPC liposome to form a stable TMB_{OX}, which was then colored and detected by UV spectrophotometer. During the experiment, 100 μL (200 $\mu g \cdot mL^{-1}$) SFAG solution was added to 600 μL PBS solution (pH 7.4), 100 μL glucose solution with different concentrations was added, and 100 m (10 mM) TMB solution were added in order. After 30 minutes of reaction, measured the absorption spectrum at 652 nm under the UV spectrophotometer and record the data. The process of detecting glucose in synthetic blood was similar to that of described above. Synthetic blood (from Leagene Biotechnology GB 19083 of China) was100-fold diluted by ultrapure water.

References:

1 P. B. Muller, R. Barnkob, M. J. Jensen and H. Bruus, *Lab Chip*, 2012, **12**, 4617-4627.

2 Gu Y, Chen C, Wang Z, et al. Plastic-based acoustofluidic devices for high-throughput, biocompatible platelet separation[J]. *Lab on a Chip*, 2019, 19(3): 394-402.

3 P. Li, T. J. Huang, *Anal. Chem.*, 2018, **91**, 757–767.

4 T. Yamamoto, K. Kubo, SV. Komarov, *Ultrason. Sonochem.*, 2021, **71**, 105381.

5 F. G. Mitri, *Ultrasonics*, 2017, **74**, 62-71.

6 Y. Qiao, X. Zhang, G. Zhang, J., Acoust. *Soc. Am.*, 2017, **141**, 4633.

7 T. Hasegawa, K. Saka, N. Inoue, K. Matsuzawa, J. Acoust. *Soc. Am.*, 1988, **83**, 1770-1775.

8 A. P. Sarvazyan, O. V. Rudenko, W. L. Nyborg, *Ultrasound Med. Biol.*, 2010, 36, 1379-1394.

9 Y. Zhou, Z. Ma, Y. Ai, *Anal. Chem.*, 2020, **92**, 12795-12800.

10 P. L. Marston, J. Acoust. *Soc. Am.*, 2013, **133**: 3237.

11 P B Muller, R Barnkob, M. J. H Jensen, H. A. Bruus, *Lab on a Chip*, 2012, **12**, 4617-4627.

12 J. Lei, *Microfluidic nanofluidics*, 2017, **21**, 50.1-50.15.

13 T. Laurell, A. Lenshof, *Lab Chip*. 2014, **10**, 29-45.

14 M. E. Gurtin, E. Fried, L. Anand, *Cambridge University Press*, 2010.

15 D. L. Miller, N. B. Smith, M. R. Bailey, G. J. Czarnota, K. Hynynen, I. R. Makin. *J. Ultrasound Med.*, 2012, **31**, 623-634.

16 S. Vincenzi, A. J. Crivelli, D. Jesensek, L. G. De, *Oecologia*., 2008, **156**, 523-534.

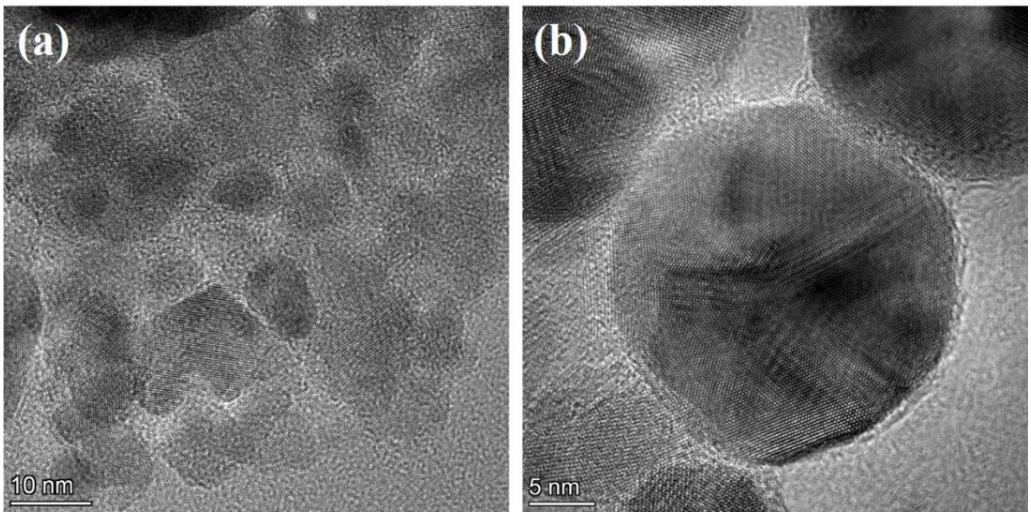

Fig. S1 TEM imagines of (a) Fe_3O_4 NPs, (b) Ag NPs.

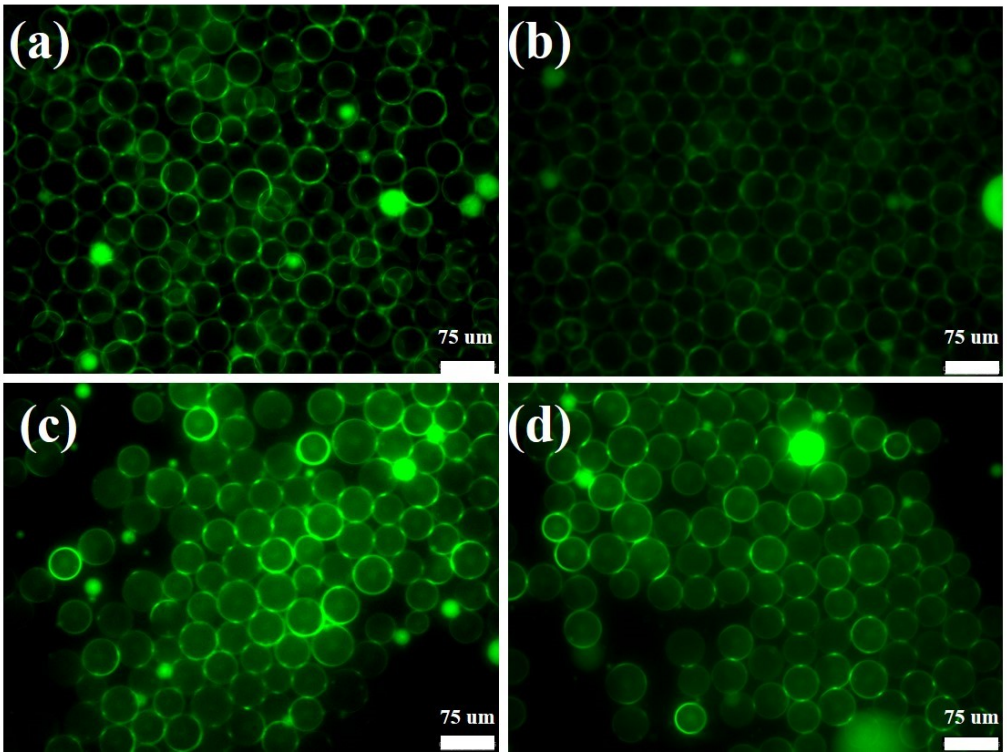

Fig. S2 (a-d) The fluorescent microscopic images of SPC liposomes.

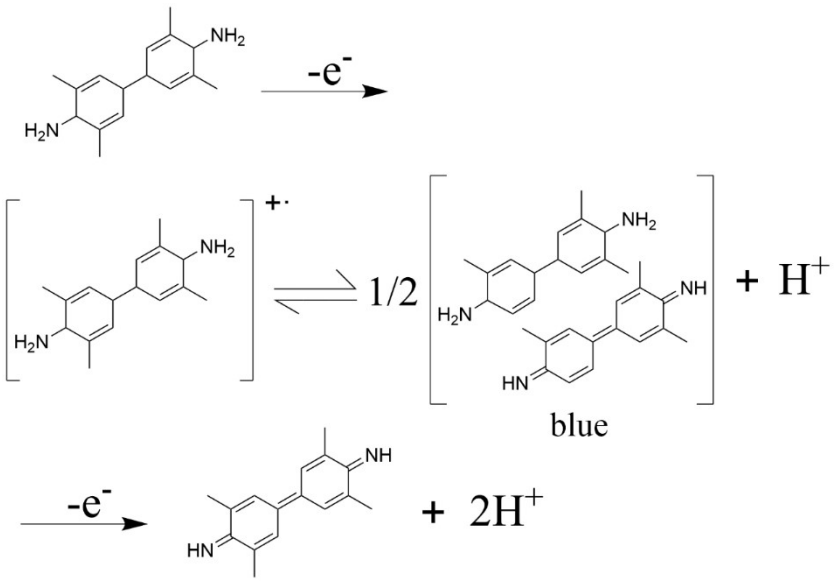

Fig. S3 Mechanism of oxidation of TMB.

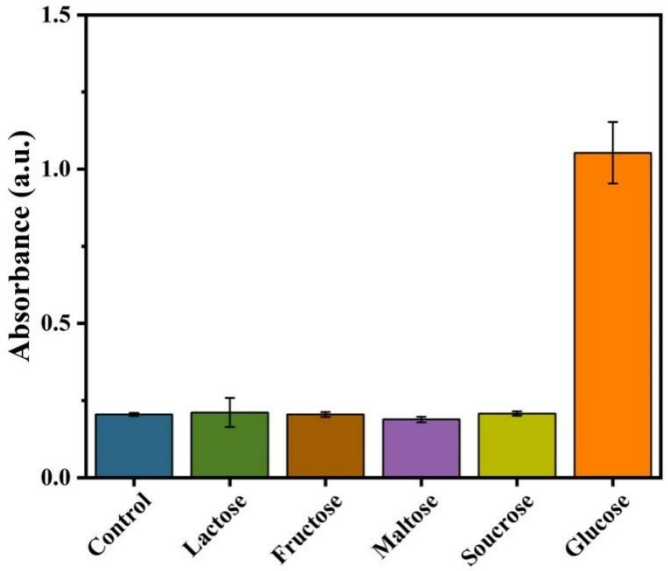

Fig. S4 The selectivity of SFAG for glucose detection by measuring the absorbance at 652 nm.

Tab. S1 Comparison of the glucose results obtained by this colormetric method and actual added glucose concentration.

Sample	Added glucose (μM)	Measured after addition (μM)	Recovery (%)
A	20	25.09	125.45
B	200	242.14	121.07
C	300	280.83	93.61